Some Alternative Forms of Nonviscous Damping

Theodore L. Chang[a,*], Chin-Long Lee[b]

[a] *IRIS Adlershof, Humboldt-Universität zu Berlin, Berlin, Germany, 12489.*
[b] *Department of Civil and Environmental Engineering, University of Canterbury, Christchurch, New Zealand, 8041.*

Abstract

This paper develops a general framework for nonviscous damping in dynamic systems by introducing additive energy-dissipating forces governed by first-order differential equations. Several choices of the driving field are examined, including displacement-, velocity-, and acceleration-dependent forms associated with stiffness and mass contributions. For each formulation, the frequency-domain response is derived to identify the corresponding storage and loss stiffnesses, admissible complex conjugate parameter pairs, stability and dissipation requirements, and asymptotic behaviour. The analysis shows that some direct formulations must be augmented by algebraic correction terms to recover the correct static stiffness, while reciprocal formulations can be converted into each other through transformed damping parameters. A trapezoidal update of the damping history variables is then embedded into a standard direct integration workflow, yielding a modified residual and a consistent tangent effective stiffness without increasing the size of the original system. Numerical examples involving single-degree-of-freedom oscillators, broadband damping approximations, and a large finite element model verify the equivalence of selected formulations, demonstrate second-order convergence, and illustrate the computational advantages and practical limitations of the proposed alternatives.

Keywords: nonviscous damping, direct integration

Numerical models of structures commonly require a damping model to represent sources of energy dissipation that are not modelled explicitly [1, 2]. Major energy dissipation associated with material hysteresis, inelastic structural response, and supplemental damping devices can often be represented directly, while additional dissipation may arise from mechanisms that are difficult to identify or quantify individually. These may include interaction between structural and non-

* corresponding author
Email address: tlcfem@gmail.com (Theodore L. Chang)

structural components, friction and contact, components idealised as elastic, and other unmodelled structural and foundation effects. A damping model is therefore commonly introduced to represent the combined effect of these unmodelled or inherent sources of energy dissipation.

The representation of such energy dissipation is not unique. In practical finite element analysis, viscous damping models have traditionally been widely used because of their mathematical simplicity and efficiency with standard time integration procedures. The Rayleigh damping model [3] is perhaps the most common example, but its frequency dependence and tendency to generate spurious damping forces in nonlinear analysis are well known to require careful treatment [4–15]. A number of alternative viscous damping formulations have therefore been developed to provide greater flexibility in controlling the distribution of damping over frequency and in reducing unintended damping effects [16, 17].

Recent developments of the bell-shaped damping model have further demonstrated that viscous damping can be constructed to satisfy a range of different modelling requirements [15, 16, 18–20]. These studies have considered the representation of prescribed frequency-dependent damping ratios, the treatment of nonlinear and softening response, the control of damping forces outside the frequency range of interest, and the formulation of damping at structural, elemental and material levels [17, 21, 22].

Nonviscous damping provides another route for representing unmodelled energy dissipation. In a nonviscous model, the dissipative force depends on the history of the response and may be expressed through hereditary relations, convolution integrals [23–30], or equivalent internal-variable formulations [31]. When suitable kernel functions are adopted, the hereditary terms can also be represented by first-order internal variables, allowing the models to be incorporated efficiently into time-domain dynamic analysis [31].

Huang et al. [32] proposed a nonviscous damping formulation based on filtering the material constitutive forces and showed that an approximately uniform loss factor could be obtained over a prescribed frequency range. This formulation, referred to by them as the uniform damping model, provides an attractive means of introducing rate-independent dissipation into nonlinear finite element analysis. More recent work has also considered efficient numerical implementations of this class of models using exponential kernels or first-order internal variables [31].

The formulation proposed by Huang et al. [32], however, represents only one possible mathematical construction for achieving the prescribed loss-factor distribution. A specified damping or loss-factor distribution defines the desired dissipative behaviour, but does not necessarily determine a unique mathematical representation of that behaviour. This raises a more fundamental question: how broad is the family of nonviscous formulations capable of reproducing the same loss-factor characteristics, and what additional properties distinguish formulations that are equivalent in their dissipative response?

This distinction is important because formulations that produce the same or similar loss-factor distributions may nevertheless differ in other respects. In particular, they may exhibit different storage stiffnesses, static limits, high- and low-frequency asymptotic behaviour, stability properties, and numerical implementation characteristics. Some formulations may also require correction terms to recover the appropriate static stiffness, while others may admit reciprocal or alternative representations that are mathematically equivalent but computationally different. Identifying these relationships helps to separate the essential dissipative behaviour from the particular mathematical form used to realise it.

This paper develops a unified framework for constructing and analysing several alternative nonviscous damping formulations. Additive energy-dissipating forces governed by first-order differential equations are introduced, with different choices of the driving field, including displacement-, velocity-, and acceleration-dependent forms associated with stiffness and mass contributions. The resulting formulations are examined in the frequency domain to determine their storage and loss stiffnesses, admissible pairs of complex parameters, stability requirements, asymptotic behaviour, and relationships with one another.

Particular attention is given to reciprocal formulations and to the correction terms required to preserve the appropriate static stiffness. These observations lead to practical formulations that retain the size of the original dynamic system and can be incorporated into standard direct integration procedures through a modified residual and consistent tangent effective stiffness. Numerical examples are then used to verify the theoretical results, demonstrate equivalence among selected formulations, and assess computational performance in a large finite element model.

1. A General Nonviscous Damping Formulation

Consider the general equation of motion of a dynamic system under an external load $\boldsymbol{p}(t)$,

$$\boldsymbol{r}(\boldsymbol{u}, \boldsymbol{v}, \boldsymbol{a}) = \boldsymbol{p}(t), \tag{1}$$

where $\boldsymbol{r} = \boldsymbol{r}(\boldsymbol{u}, \boldsymbol{v}, \boldsymbol{a})$ is the overall resistance of the system, accounting for contributions from displacement $\boldsymbol{u}$, velocity $\boldsymbol{v}$ and acceleration $\boldsymbol{a}$. Assuming that the contributions of $\boldsymbol{u}$, $\boldsymbol{v} = \dot{\boldsymbol{u}}$, and $\boldsymbol{a} = \ddot{\boldsymbol{u}}$ are separable, there is no coupling among them, the resistance $\boldsymbol{r}$ can be then divided into three components

$$\boldsymbol{r} = \boldsymbol{r}_{\boldsymbol{u}} + \boldsymbol{r}_{\boldsymbol{v}} + \boldsymbol{r}_{\boldsymbol{a}}, \tag{2}$$

where $\boldsymbol{r}_{\aleph} = \boldsymbol{r}_{\aleph}(\aleph)$ is a function of $\aleph \in \{\boldsymbol{u}, \boldsymbol{v}, \boldsymbol{a}\}$. Additional energy-dissipating terms can be introduced, for example,

$$\boxed{\boldsymbol{r} + \boldsymbol{f} = \boldsymbol{p},} \tag{3}$$

where $\boldsymbol{f}$ can be additively decomposed as

$$\boldsymbol{f} = \sum \boldsymbol{f}_j. \tag{4}$$

Each term $\boldsymbol{f}_j$ is assumed to be governed by a first-order differential equation such that

$$g\left(\dot{\boldsymbol{f}}_j, \boldsymbol{f}_j, \boldsymbol{y}_j\right) = \boldsymbol{0}, \tag{5}$$

where $\boldsymbol{y}_j = \boldsymbol{y}_j(\boldsymbol{u}, \boldsymbol{v}, \boldsymbol{a})$ is an internal field.

For simplicity, throughout this work we assume that each $\boldsymbol{f}_j$ is governed by the following linear differential equation:

$$\dot{\boldsymbol{f}}_j = -s_j \boldsymbol{f}_j + m_j \boldsymbol{y}_j \tag{6}$$

where $s_j \in \mathbb{R}$ and $m_j \in \mathbb{R}$ are distinct real scalar parameters that control the response. Both can be extended to the complex domain $\mathbb{C}$ subject to additional conditions, as discussed below. To ensure stability, the poles s_j must satisfy the necessary condition $\Re\left(s_j\right) > 0$. It is also assumed that the initial condition for $\boldsymbol{f}_j$ is trivial; that is, $\boldsymbol{f}_j\left(0\right) = \boldsymbol{0}$.

1.1. Formulation 1

For ease of discussion, we consider the linear version of Eq. (3) under free vibration ($\boldsymbol{p} = \boldsymbol{0}$), which is

$$\begin{cases} \boldsymbol{M}\ddot{\boldsymbol{u}} + \boldsymbol{K}\boldsymbol{u} + \sum \boldsymbol{f}_j = \boldsymbol{0}, \\ \dot{\boldsymbol{f}}_j = -s_j\boldsymbol{f}_j + m_j\boldsymbol{K}\boldsymbol{u}, \end{cases} \tag{7}$$

with $\boldsymbol{y}_j = \boldsymbol{K}\boldsymbol{u}$ and real parameters s_j and m_j. Assuming harmonic solutions for both $\boldsymbol{u}$ and $\boldsymbol{f}_j$,

$$\boldsymbol{u}\left(t\right) = \boldsymbol{U}\left(\omega\right)\exp\left(i\omega t\right), \qquad \boldsymbol{f}_j\left(t\right) = \boldsymbol{F}_j\left(\omega\right)\exp\left(i\omega t\right), \tag{8}$$

the second expression can be written in the frequency domain as

$$i\omega\boldsymbol{F}_j = -s_j\boldsymbol{F}_j + m_j\boldsymbol{K}\boldsymbol{U}, \tag{9}$$

so that $\boldsymbol{F}_j = \dfrac{m_j}{s_j + i\omega}\boldsymbol{K}\boldsymbol{U}$. Substituting it back to the first expression, the characteristic equation can then be derived as

$$\det\left(\left(1 + \sum\frac{m_j}{s_j + i\omega}\right)\boldsymbol{K} - \omega^2\boldsymbol{M}\right) = 0. \tag{10}$$

The dynamic stiffness $\boldsymbol{K}^*$ is

$$\boldsymbol{K}^* = \left(1 + \sum\frac{m_j}{s_j + i\omega}\right)\boldsymbol{K} \tag{11}$$

with storage stiffness $\boldsymbol{K}'$ and loss stiffness $\boldsymbol{K}''$

$$\boldsymbol{K}' = \left(1 + \sum\frac{s_j m_j}{s_j^2 + \omega^2}\right)\boldsymbol{K}, \qquad \boldsymbol{K}'' = -\sum\frac{m_j\omega}{s_j^2 + \omega^2}\boldsymbol{K} \tag{12}$$

such that $\boldsymbol{K}^* = \boldsymbol{K}' + \boldsymbol{K}''i$. The limiting cases are

$$\lim_{\omega\to 0} \boldsymbol{K}' = \left(1 + \sum \frac{m_j}{s_j}\right)\boldsymbol{K}, \qquad \lim_{\omega\to\infty} \boldsymbol{K}' = \boldsymbol{K}. \tag{13}$$

In this formulation, $m_j < 0$ is required to ensure that the system is dissipative. Physically, $\boldsymbol{f}_j$ represent filtered hysteretic resistance forces and must be exerted against motion in order to dissipate energy. Accordingly, the storage stiffness $\boldsymbol{K}'$ softens at low frequencies (since $m_j < 0$ and $s_j > 0$) and approaches the original stiffness $\boldsymbol{K}$ at high frequencies.

1.2. Guaranteed Energy Dissipation

The choice $\boldsymbol{y}_j = \boldsymbol{K}\boldsymbol{u}$ yields a dynamic stiffness proportional to the exact stiffness matrix $\boldsymbol{K}$, enabling the definition of a scalar loss ratio and, potentially, an equivalent damping factor. However, for systems exhibiting stiffness degradation or damage induced softening, this formulation may inject energy into the system rather than dissipate it.

To ensure a dissipative system, repeating this procedure with $\boldsymbol{y}_j = \boldsymbol{u}$ gives the following stiffnesses:

$$\boldsymbol{K}' = \boldsymbol{K} + \sum \frac{s_j m_j}{s_j^2 + \omega^2}\boldsymbol{I}, \qquad \boldsymbol{K}'' = -\sum \frac{m_j \omega}{s_j^2 + \omega^2}\boldsymbol{I}. \tag{14}$$

Under this choice, the loss stiffness $\boldsymbol{K}''$ becomes independent of the static stiffness $\boldsymbol{K}$. Although a scalar loss ratio can no longer be defined, the formulation guarantees positive energy dissipation.

1.3. Complex Realm Extension

The above analyses assume s_j and m_j are real scalars. If m_j and s_j come in conjugate pairs, for example,

$$\boxed{m_j \in \mathbb{C}, \qquad s_j \in \mathbb{C}, \qquad m_{j+1} = \overline{m_j}, \qquad s_{j+1} = \overline{s_j},} \tag{15}$$

then the corresponding expressions for storage and loss stiffnesses still hold. For example, the real part is

$$\begin{aligned}
&\Re\left(\frac{m_j}{s_j+i\omega}+\frac{m_{j+1}}{s_{j+1}+i\omega}\right)=\Re\left(\frac{m_j}{s_j+i\omega}+\frac{\overline{m_j}}{\overline{s_j}+i\omega}\right)\\
&=\Re\left(\frac{m_j}{s_j+i\omega}+\overline{\frac{m_j}{s_j-i\omega}}\right)=\Re\left(\frac{m_j}{s_j+i\omega}+\frac{m_j}{s_j-i\omega}\right)=\Re\left(\frac{2s_jm_j}{s_j^2+\omega^2}\right)\\
&=\Re\left(\frac{s_jm_j}{s_j^2+\omega^2}+\frac{s_jm_j}{s_j^2+\omega^2}\right)=\Re\left(\frac{s_jm_j}{s_j^2+\omega^2}+\overline{\frac{s_jm_j}{s_j^2+\omega^2}}\right)=\Re\left(\frac{s_jm_j}{s_j^2+\omega^2}+\frac{s_{j+1}m_{j+1}}{s_{j+1}^2+\omega^2}\right).
\end{aligned}\tag{16}$$

This implies that the parameters s_j and m_j can be extended to the complex domain, provided that they come in conjugate pairs. In the following, we therefore assume $s_j\in\mathbb{C}$ and $m_j\in\mathbb{C}$ with this additional constraint implied. Again, a stable system requires $\Re\left(s_j\right)>0$.

1.4. Formulation 2

Alternatively, one can pick $\boldsymbol{y}_j=\boldsymbol{M}\boldsymbol{a}$. The system becomes

$$\begin{cases}\boldsymbol{M}\ddot{\boldsymbol{u}}+\boldsymbol{K}\boldsymbol{u}+\sum\boldsymbol{f}_j=\boldsymbol{0},\\ \dot{\boldsymbol{f}}_j=-s_j\boldsymbol{f}_j+m_j\boldsymbol{M}\boldsymbol{a}.\end{cases}\tag{17}$$

Adopting a similar approach, the characteristic equation can be derived as

$$\det\left(\frac{1}{1+\sum\dfrac{m_j}{s_j+i\omega}}\boldsymbol{K}-\omega^2\boldsymbol{M}\right)=0.\tag{18}$$

The magnitude of the loss ratio remains the same because the scalar coefficient is the reciprocal of that in the previous case. In this formulation, a dissipative system requires $\Re\left(m_j\right)>0$.

It is possible to show that Eq. (18) is in fact identical to Eq. (10). Rewriting the scalar coefficient in matrix form with $\boldsymbol{s}=\begin{bmatrix}s_1 & s_2 & \cdots\end{bmatrix}^\mathrm{T}$ and $\boldsymbol{m}=\begin{bmatrix}m_1 & m_2 & \cdots\end{bmatrix}^\mathrm{T}$ and applying the Sherman–Morrison–Woodbury formula gives

$$\begin{aligned}
\frac{1}{1+\sum\dfrac{m_j}{s_j+i\omega}}&=\left(1+\boldsymbol{1}^\mathrm{T}\mathrm{diag}\left(\boldsymbol{s}+i\omega\right)^{-1}\boldsymbol{m}\right)^{-1}\\
&=1-\boldsymbol{1}^\mathrm{T}\left(\mathrm{diag}\left(\boldsymbol{s}+i\omega\right)+\boldsymbol{m}\boldsymbol{1}^\mathrm{T}\right)^{-1}\boldsymbol{m}.
\end{aligned}\tag{19}$$

Assuming the matrix $\operatorname{diag}(\boldsymbol{s})+\boldsymbol{m}\boldsymbol{1}^\mathrm{T}$ is neither defective nor degenerate, which is always possible by carefully selecting parameters s_j and m_j, and denoting its eigenvalues as s'_j and the corresponding left and right eigenvectors as $\boldsymbol{\phi}^l_j$ and $\boldsymbol{\phi}^r_j$, then

$$\frac{1}{1+\sum\dfrac{m_j}{s_j+i\omega}}=1+\sum\frac{m'_j}{s'_j+i\omega}\qquad\text{with}\quad m'_j=-\frac{\left\langle\boldsymbol{1},\boldsymbol{\phi}^r_j\right\rangle\left\langle\boldsymbol{\phi}^l_j,\boldsymbol{m}\right\rangle}{\left\langle\boldsymbol{\phi}^r_j,\boldsymbol{\phi}^l_j\right\rangle}.\tag{20}$$

For suitable sets of s_j and m_j, it is thus possible to find the corresponding sets s'_j and m'_j to convert between Eq. (18) and Eq. (10). This process naturally extends the definition of s_j and m_j to the complex domain. Even if the input pairs are real, for example, $s_j, m_j \in \mathbb{R}$, the corresponding s'_j and m'_j can be complex because s'_j, which are eigenvalues of the matrix $\operatorname{diag}(\boldsymbol{s})+\boldsymbol{m}\boldsymbol{1}^\mathrm{T}$, are not necessarily real. In the absence of other energy-dissipating actions, the two formulations are thus equivalent. This equivalence may offer numerical advantages when the mass matrix is constant, as is often the case, and more sparse than the stiffness matrix, particularly under a lumped mass formulation. Note that this equivalence is only valid under free vibration. For forced vibration, the external load $\boldsymbol{p}$ must be properly transformed to ensure the same equivalence, see later discussions.

1.5. Wrong Asymptotic Behaviour

The fundamental consistency requirement states that $\boldsymbol{K}^*$ (or $\boldsymbol{K}'$) must approach the static stiffness $\boldsymbol{K}$ at low frequencies, that is, $\lim\limits_{\omega\to0}\boldsymbol{K}^*=\boldsymbol{K}$, to ensure the system behaves as expected under (quasi-)static loading conditions. However, $\boldsymbol{K}'$ fails to meet this requirement in Eq. (12). The formulation must therefore be augmented to fix this issue, for example, by introducing non-trivial terms $\boldsymbol{h}_j$ to cancel the contribution of $\sum\dfrac{m_j}{s_j}\boldsymbol{K}$ at low frequencies, resulting in

$$\begin{cases}\boldsymbol{M}\ddot{\boldsymbol{u}}+\boldsymbol{K}\boldsymbol{u}+\sum\boldsymbol{f}_j+\sum\boldsymbol{h}_j=\boldsymbol{0},\\ \dot{\boldsymbol{f}}_j=-s_j\boldsymbol{f}_j+m_j\boldsymbol{K}\boldsymbol{u},\\ s_j\boldsymbol{h}_j=-m_j\boldsymbol{K}\boldsymbol{u}.\end{cases}\tag{21}$$

The corresponding dynamic stiffness $\boldsymbol{K}^*$ is

$$\boldsymbol{K}^*=\left(1-\sum\frac{m_j}{s_j}+\sum\frac{m_j}{s_j+i\omega}\right)\boldsymbol{K}=\left(1-\sum\frac{m_j}{s_j}\frac{i\omega}{s_j+i\omega}\right)\boldsymbol{K}\tag{22}$$

with storage stiffness $\boldsymbol{K}'$ and loss stiffness $\boldsymbol{K}''$

$$\boldsymbol{K}' = \left(1 - \sum \frac{m_j}{s_j} + \sum \frac{s_j m_j}{s_j^2 + \omega^2}\right)\boldsymbol{K}, \qquad \boldsymbol{K}'' = -\sum \frac{m_j \omega}{s_j^2 + \omega^2}\boldsymbol{K}. \tag{23}$$

With this modification,

$$\lim_{\omega\to 0} \boldsymbol{K}' = \boldsymbol{K}, \qquad \lim_{\omega\to\infty} \boldsymbol{K}' = \left(1 - \sum \frac{m_j}{s_j}\right)\boldsymbol{K}. \tag{24}$$

Due to equivalence, the formulation in § 1.4 also does not meet the consistency requirement. A similar modification shall be applied. Only the governing system is presented below, without repeating the lengthy derivations.

$$\begin{cases} \boldsymbol{M}\ddot{\boldsymbol{u}} + \boldsymbol{K}\boldsymbol{u} + \sum \boldsymbol{f}_j + \sum \boldsymbol{h}_j = \boldsymbol{0}, \\ \dot{\boldsymbol{f}}_j = -s_j \boldsymbol{f}_j + m_j \boldsymbol{M}\boldsymbol{a}, \\ s_j \boldsymbol{h}_j = -m_j \boldsymbol{M}\boldsymbol{a}. \end{cases} \tag{25}$$

1.6. Formulation 3

We now consider $\boldsymbol{y}_j = \boldsymbol{K}\boldsymbol{v}$, for which the system becomes

$$\begin{cases} \boldsymbol{M}\ddot{\boldsymbol{u}} + \boldsymbol{K}\boldsymbol{u} + \sum \boldsymbol{f}_j = \boldsymbol{0}, \\ \dot{\boldsymbol{f}}_j = -s_j \boldsymbol{f}_j + m_j \boldsymbol{K}\dot{\boldsymbol{u}}. \end{cases} \tag{26}$$

The characteristic equation can be derived as

$$\det\left(\left(1 + \sum \frac{m_j i\omega}{s_j + i\omega}\right)\boldsymbol{K} - \omega^2 \boldsymbol{M}\right) = 0. \tag{27}$$

Thus,

$$\boldsymbol{K}' = \left(1 + \sum \frac{m_j \omega^2}{s_j^2 + \omega^2}\right)\boldsymbol{K}, \qquad \boldsymbol{K}'' = \sum \frac{s_j m_j \omega}{s_j^2 + \omega^2}\boldsymbol{K}. \tag{28}$$

The limiting cases are

$$\lim_{\omega\to 0} \boldsymbol{K}' = \boldsymbol{K}, \qquad \lim_{\omega\to\infty} \boldsymbol{K}' = \left(1 + \sum m_j\right)\boldsymbol{K}. \tag{29}$$

In this formulation, a dissipative system requires $\Re\left(m_j\right) > 0$. The loss stiffness $\boldsymbol{K}''$ in this case is positive, indicating that the system is dissipative and stable when $\Re\left(m_j\right) > 0$. Unlike the previous formulations, the storage stiffness $\boldsymbol{K}'$ approaches the original stiffness $\boldsymbol{K}$ at low frequencies and hardens at high frequencies.

It is equivalent to Eq. (21) after a simple parameter mapping: s_j stays unchanged, and replacing m_j in Eq. (26) by $-m_j/s_j$ yields Eq. (21). By comparing Eq. (21) and Eq. (26), one can also derive the following third identical formulation.

$$\begin{cases} \boldsymbol{M}\ddot{\boldsymbol{u}} + \boldsymbol{K}\boldsymbol{u} - \sum \dfrac{\dot{\boldsymbol{f}}_j}{s_j} = \boldsymbol{0}, \\ \dot{\boldsymbol{f}}_j = -s_j\boldsymbol{f}_j + m_j\boldsymbol{K}\boldsymbol{u}. \end{cases} \tag{30}$$

A careful comparison reveals that Eq. (30) is equivalent to the model by Huang et al. [32], which adopts real parameters s_j and m_j. One shall see that in essence this formulation applies an energy-dissipating force $\boldsymbol{f}_j$ that is the filtered version of the stiffness proportional viscous damping force $\boldsymbol{K}\dot{\boldsymbol{u}}$ (c.f., Eq. (26)).

1.7. Formulation 4

Alternatively, for $\boldsymbol{y}_j = \boldsymbol{M}\dot{\boldsymbol{a}}$, the corresponding characteristic equation can be expressed as

$$\det\left(\boldsymbol{K} - \left(1 + \sum \frac{m_j i\omega}{s_j + i\omega}\right)\omega^2\boldsymbol{M}\right) = 0, \tag{31}$$

resulting in the dynamic stiffness

$$\boldsymbol{K}^* = \frac{1}{1 + \sum \dfrac{m_j i\omega}{s_j + i\omega}}\boldsymbol{K}. \tag{32}$$

As in the previous derivation, partial fraction decomposition can be used to find s'_j and m'_j (explicit expressions are not shown for brevity) such that

$$\frac{1}{1 + \sum \dfrac{m_j i\omega}{s_j + i\omega}} = 1 + \sum \frac{m'_j i\omega}{s'_j + i\omega}. \tag{33}$$

Thus, Eq. (31) is an equivalent alternative formulation of Eq. (27). Because computing and storing $\dot{\boldsymbol{a}} = \dddot{\boldsymbol{u}}$ is typically **not** supported in analysis frameworks, this practically restrictive formulation is presented solely to establish the equivalence between the two forms. If $\ddot{\boldsymbol{u}}$ is tracked, the system can leverage the unique characteristics of the mass matrix detailed in previous sections.

1.8. Forced Vibration

If the external load $\boldsymbol{p}$ is non-trivial, consider the system Eq. (25) with $\boldsymbol{h}_j$ merged and an augmented right-hand side,

$$\begin{cases} \left(1-\sum\dfrac{m_j}{s_j}\right)\boldsymbol{M}\ddot{\boldsymbol{u}}+\boldsymbol{K}\boldsymbol{u}+\sum\boldsymbol{f}_j=\left(1-\sum\dfrac{m_j}{s_j}\right)\boldsymbol{p}+\sum\boldsymbol{q}_j,\\ \dot{\boldsymbol{f}}_j=-s_j\boldsymbol{f}_j+m_j\boldsymbol{M}\boldsymbol{a},\\ \dot{\boldsymbol{q}}_j=-s_j\boldsymbol{q}_j+m_j\boldsymbol{p}. \end{cases} \tag{34}$$

Assuming harmonic solutions for $\boldsymbol{u}=\boldsymbol{U}\left(\omega\right)\exp\left(i\omega t\right)$, $\boldsymbol{f}_j=\boldsymbol{F}_j\left(\omega\right)\exp\left(i\omega t\right)$, $\boldsymbol{q}_j=\boldsymbol{Q}_j\left(\omega\right)\exp\left(i\omega t\right)$ and $\boldsymbol{p}=\boldsymbol{P}\left(\omega\right)\exp\left(i\omega t\right)$, the equation of motion can be expressed in the frequency domain as

$$\left(\boldsymbol{K}-\left(1-\sum\frac{m_j}{s_j}+\sum\frac{m_j}{s_j+i\omega}\right)\omega^2\boldsymbol{M}\right)\boldsymbol{U}=\left(1-\sum\frac{m_j}{s_j}+\sum\frac{m_j}{s_j+i\omega}\right)\boldsymbol{P}. \tag{35}$$

It is then straightforward to rewrite Eq. (35) as

$$\begin{aligned} &\left(\frac{1}{1-\sum\dfrac{m_j}{s_j}\dfrac{i\omega}{s_j+i\omega}}\boldsymbol{K}-\omega^2\boldsymbol{M}\right)\boldsymbol{U}=\boldsymbol{P}\\ &\qquad\longrightarrow\qquad\left(\left(1-\sum\frac{m'_j}{s'_j}\frac{i\omega}{s'_j+i\omega}\right)\boldsymbol{K}-\omega^2\boldsymbol{M}\right)\boldsymbol{U}=\boldsymbol{P} \end{aligned} \tag{36}$$

using Eq. (33). This corresponds to the system Eq. (21) under forced vibration, which is

$$\begin{cases} \boldsymbol{M}\ddot{\boldsymbol{u}}+\left(1-\sum\dfrac{m_j}{s_j}\right)\boldsymbol{K}\boldsymbol{u}+\sum\boldsymbol{f}_j=\boldsymbol{p},\\ \dot{\boldsymbol{f}}_j=-s_j\boldsymbol{f}_j+m_j\boldsymbol{K}\boldsymbol{u}. \end{cases} \tag{37}$$

1.9. Remarks

Because the trivial initial condition $\boldsymbol{f}_j(0) = \boldsymbol{0}$ is assumed, the relation discussed by Chang and Lee [31] can be used to express the proposed formulations equivalently as

$$\boldsymbol{r} + \sum g_j * \boldsymbol{y}_j = \boldsymbol{p} \tag{38}$$

where $g_j * \boldsymbol{y}_j$ denotes the convolution of the kernel g_j and $\boldsymbol{y}_j$; that is,

$$(g_j * \boldsymbol{y}_j)(t) = \int_0^t g_j(t-\tau)\,\boldsymbol{y}_j(\tau)\,\mathrm{d}\tau, \tag{39}$$

with $g_j = g_j(t) = m_j \exp(-s_j t)$ and $\boldsymbol{y}_j$ taking one of the forms discussed above. This type of equivalence provides an alternative perspective to understand various damping formulations. The damping characteristics, parametrised by s_j and m_j, may be interpreted as modifications to the kernel functions g_j, enabling the desired damping response to be realised through kernel design.

Among the formulations above, three practical variants are restated in the nonlinear context as follows. They are equivalent to one another and yield identical energy dissipation characteristics, provided that the parameters s_j and m_j are properly adjusted.

UDD — Displacement Dependent. This formulation requires scaling of the tangent stiffness matrix $\boldsymbol{K}$. From an implementation perspective, this operation might be mitigated by applying the reciprocal of the scaling factor to the rest components in the equation, namely matrices that already require scaling or vectors that are inexpensive to compute. Its computational cost is lower than that of Eq. (41), while remaining comparable to that of Eq. (42), being potentially slightly higher or lower depending on the implementation details and configuration.

$$\boxed{\begin{cases} \boldsymbol{r}_{\boldsymbol{a}} + \boldsymbol{r}_{\boldsymbol{v}} + \left(1 - \sum \dfrac{m_j}{s_j}\right)\boldsymbol{r}_{\boldsymbol{u}} + \sum \boldsymbol{f}_j = \boldsymbol{p}, \\ \dot{\boldsymbol{f}}_j = -s_j \boldsymbol{f}_j + m_j \boldsymbol{r}_{\boldsymbol{u}}. \end{cases}} \tag{40}$$

UDV — Velocity Dependent. This formulation also requires scaling of the tangent stiffness matrix $\boldsymbol{K}$. In addition, the non-standard quantity $\boldsymbol{K}\boldsymbol{v}$ must be computed, assembled, and stored as an additional history variable, resulting in the highest computational cost among the three formulations although its analytical form is the most concise one.

$$\boxed{\begin{cases} \boldsymbol{r_a}+\boldsymbol{r_v}+\boldsymbol{r_u}+\sum\boldsymbol{f}_j=\boldsymbol{p},\\ \dot{\boldsymbol{f}}_j=-s_j\boldsymbol{f}_j+m_j\dot{\boldsymbol{r}}_{\boldsymbol{u}}. \end{cases}}\tag{41}$$

UDA — Acceleration Dependent. This formulation requires scaling of the mass matrix $\boldsymbol{M}$. Since $\boldsymbol{M}$ is typically sparser than $\boldsymbol{K}$ and must be scaled regardless in displacement based dynamic analyses, the additional computational cost is negligible. This formulation tracks two internal fields $\boldsymbol{f}_j$ and $\boldsymbol{q}_j$ instead of one in the other two formulations.

$$\boxed{\begin{cases} \left(1-\sum\dfrac{m_j}{s_j}\right)\boldsymbol{r_a}+\boldsymbol{r_v}+\boldsymbol{r_u}+\sum\boldsymbol{f}_j=\left(1-\sum\dfrac{m_j}{s_j}\right)\boldsymbol{p}+\sum\boldsymbol{q}_j,\\ \dot{\boldsymbol{f}}_j=-s_j\boldsymbol{f}_j+m_j\boldsymbol{r_a},\\ \dot{\boldsymbol{q}}_j=-s_j\boldsymbol{q}_j+m_j\boldsymbol{p}. \end{cases}}\tag{42}$$

2. Numerical Implementation

2.1. The General System

The algorithm discussed in the previous work [31] is repurposed here to handle various types of systems. In the general nonlinear context, the governing system is

$$\begin{cases} \dot{\boldsymbol{f}}_j=-s_j\boldsymbol{f}_j+m_j\boldsymbol{y}_j,\\ \boldsymbol{r}+\sum\boldsymbol{f}_j+\sum\boldsymbol{h}_j=\boldsymbol{z}. \end{cases}\tag{43}$$

Because the external load $\boldsymbol{p}$ may be augmented as in Eq. (42), $\boldsymbol{z}$ is used here instead.

2.1.1. Effective Stiffness

The first expression is a first-order ODE for $\boldsymbol{f}_j$ that can be integrated with the implicit trapezoidal rule, which is second-order accurate and A-stable,

$$\boldsymbol{f}_{j,n+1}=\boldsymbol{f}_{j,n}+\frac{\Delta t}{2}\left(\dot{\boldsymbol{f}}_{j,n}+\dot{\boldsymbol{f}}_{j,n+1}\right).\tag{44}$$

Expanding gives

$$\boldsymbol{f}_{j,n+1} = \boldsymbol{f}_{j,n} + \frac{\Delta t}{2}\left(\left(-s_j \boldsymbol{f}_{j,n} + m_j \boldsymbol{y}_{j,n}\right) + \left(-s_j \boldsymbol{f}_{j,n+1} + m_j \boldsymbol{y}_{j,n+1}\right)\right), \tag{45}$$

which can be rearranged to obtain

$$\boldsymbol{f}_{j,n+1} = \frac{2 - s_j \Delta t}{2 + s_j \Delta t} \boldsymbol{f}_{j,n} + \frac{m_j \Delta t}{2 + s_j \Delta t} \boldsymbol{y}_{j,n} + \frac{m_j \Delta t}{2 + s_j \Delta t} \boldsymbol{y}_{j,n+1}, \tag{46}$$

in which subscripts $(\cdot)_n$ and $(\cdot)_{n+1}$ denote the corresponding quantity at t_n and $t_{n+1} = t_n + \Delta t$.

Assuming that the equation of motion (equilibrium) is satisfied at t_{n+1}, which is valid for a wide range of time integration methods (including the well-known Newmark method), the second expression is

$$\boldsymbol{r}_{n+1} + \sum \frac{2 - s_j \Delta t}{2 + s_j \Delta t} \boldsymbol{f}_{j,n} + \sum \frac{m_j \Delta t}{2 + s_j \Delta t} \boldsymbol{y}_{j,n} + \sum \frac{m_j \Delta t}{2 + s_j \Delta t} \boldsymbol{y}_{j,n+1} + \sum \boldsymbol{h}_{j,n+1} = \boldsymbol{z}_{n+1}. \tag{47}$$

Differentiation leads to the following revised effective stiffness $\hat{\boldsymbol{K}}_{n+1}$,

$$\hat{\boldsymbol{K}}_{n+1} = \bar{\boldsymbol{K}}_{n+1} + \sum \frac{m_j \Delta t}{2 + s_j \Delta t} \frac{\mathrm{d}\boldsymbol{y}_{j,n+1}}{\mathrm{d}\boldsymbol{u}_{n+1}} + \sum \frac{\mathrm{d}\boldsymbol{h}_{j,n+1}}{\mathrm{d}\boldsymbol{u}_{n+1}}. \tag{48}$$

where the conventional effective stiffness $\bar{\boldsymbol{K}}_{n+1}$ is

$$\bar{\boldsymbol{K}}_{n+1} = \frac{\mathrm{d}\boldsymbol{r}_{n+1}}{\mathrm{d}\boldsymbol{u}_{n+1}} = \boldsymbol{K}_{n+1} + \boldsymbol{C}_{n+1} \frac{\mathrm{d}\boldsymbol{v}_{n+1}}{\mathrm{d}\boldsymbol{u}_{n+1}} + \boldsymbol{M}_{n+1} \frac{\mathrm{d}\boldsymbol{a}_{n+1}}{\mathrm{d}\boldsymbol{u}_{n+1}}. \tag{49}$$

In this work, we have considered two options: the trivial case $\boldsymbol{h}_j = \boldsymbol{0}$ that corresponds to Eq. (41) and the non-trivial case $\boldsymbol{h}_j = -\dfrac{m_j}{s_j} \boldsymbol{y}_j$ that corresponds to Eq. (40) and Eq. (42). For the latter,

$$\sum \frac{\mathrm{d}\boldsymbol{h}_{j,n+1}}{\mathrm{d}\boldsymbol{u}_{n+1}} = -\sum \frac{m_j}{s_j} \frac{\mathrm{d}\boldsymbol{y}_{j,n+1}}{\mathrm{d}\boldsymbol{u}_{n+1}} \tag{50}$$

can be combined with the second term in Eq. (48).

It follows from Eq. (48) that accounting for this energy-dissipating action requires adding only the matrix $\sum \dfrac{m_j \Delta t}{2 + s_j \Delta t} \dfrac{\mathrm{d}\boldsymbol{y}_{j,n+1}}{\mathrm{d}\boldsymbol{u}_{n+1}}$, or $\sum \left(\dfrac{m_j \Delta t}{2 + s_j \Delta t} - \dfrac{m_j}{s_j}\right) \dfrac{\mathrm{d}\boldsymbol{y}_{j,n+1}}{\mathrm{d}\boldsymbol{u}_{n+1}}$ if $\boldsymbol{h}_j$ is present, to the original effective stiffness $\bar{\boldsymbol{K}}_{n+1}$. In certain cases, this additional matrix can be formed very efficiently. For example, if $\boldsymbol{y}_j \in \{\boldsymbol{r_u}, \boldsymbol{r_a}\}$, then $\dfrac{\mathrm{d}\boldsymbol{y}_{j,n+1}}{\mathrm{d}\boldsymbol{u}_{n+1}}$ is simply the (possibly scaled) stiffness matrix $\boldsymbol{K}_{n+1}$ (or the mass matrix $\boldsymbol{M}_{n+1}$) that is already available in the original formulation. In other special cases, this matrix can be diagonal; for example, with $\boldsymbol{y}_j \in \{\boldsymbol{u}, \boldsymbol{v}, \boldsymbol{a}\}$, $\dfrac{\mathrm{d}\boldsymbol{y}_{j,n+1}}{\mathrm{d}\boldsymbol{u}_{n+1}} = \alpha\boldsymbol{I}$ is a diagonal matrix with a possibly non-unit scalar α. Adding such a diagonal matrix to $\hat{\boldsymbol{K}}_{n+1}$ is almost computationally trivial.

2.1.2. Effective Load

For Eq. (40) and Eq. (41), the effective load is simply

$$\boldsymbol{z}_{n+1} = \boldsymbol{p}_{n+1}. \tag{51}$$

In Eq. (42), applying the same trapezoidal rule, one obtains

$$\boldsymbol{q}_{j,n+1} = \frac{2 - s_j\Delta t}{2 + s_j\Delta t}\boldsymbol{q}_{j,n} + \frac{m_j\Delta t}{2 + s_j\Delta t}\boldsymbol{p}_n + \frac{m_j\Delta t}{2 + s_j\Delta t}\boldsymbol{p}_{n+1}, \tag{52}$$

thus

$$\begin{aligned}\boldsymbol{z}_{n+1} &= \left(1 - \sum\frac{m_j}{s_j}\right)\boldsymbol{p}_{n+1} + \sum\boldsymbol{q}_{j,n+1}\\ &= \sum\frac{2 - s_j\Delta t}{2 + s_j\Delta t}\boldsymbol{q}_{j,n} + \sum\frac{m_j\Delta t}{2 + s_j\Delta t}\boldsymbol{p}_n + \left(1 - \sum\frac{m_j}{s_j} + \sum\frac{m_j\Delta t}{2 + s_j\Delta t}\right)\boldsymbol{p}_{n+1}.\end{aligned} \tag{53}$$

2.1.3. A Reference Algorithm

Algorithm 1 presents an algorithm that integrates the proposed damping formulation into an existing iterative analysis workflow. The subscript $(\cdot)_{n+1}$ is dropped for brevity. Once convergence is achieved, $\boldsymbol{f}_{j,n} \leftarrow \boldsymbol{f}_j$ and $\boldsymbol{q}_{j,n} \leftarrow \boldsymbol{q}_j$ are committed. When $\boldsymbol{h}_j$ is an algebraic function of $\boldsymbol{y}_j$, there is usually no need to store it separately. Even though $\boldsymbol{f}_j$ can be complex due to complex s_j and m_j, as long as conjugate pairs of s_j and m_j are used, $\boldsymbol{f} = \sum\boldsymbol{f}_j$ and $\boldsymbol{q} = \sum\boldsymbol{q}_j$ are real-valued. The same applies to the scalars $\sum\dfrac{m_j\Delta t}{2 + s_j\Delta t}$ and $\sum\dfrac{m_j}{s_j}$, and thus $\hat{\boldsymbol{K}}$ is real-valued.

Algorithm 1 iteration body of solving dynamic systems with general damping

***Schema: Newmark + Trapezoidal**

Input: $\bar{\boldsymbol{K}}$, $\boldsymbol{u}$, $\boldsymbol{v}$, $\boldsymbol{a}$, $\boldsymbol{r}$, $\boldsymbol{p}$ (quantities obtained in the conventional manner as if there is no general damping); damping history/parameters $\boldsymbol{f}_{j,n}$, $\boldsymbol{y}_{j,n}$, $\boldsymbol{q}_{j,n}$, m_j, s_j

Output: $\boldsymbol{u}$

compute energy-dissipating force $\boldsymbol{f}_j = \dfrac{2 - s_j\Delta t}{2 + s_j\Delta t}\boldsymbol{f}_{j,n} + \dfrac{m_j\Delta t}{2 + s_j\Delta t}\boldsymbol{y}_{j,n} + \dfrac{m_j\Delta t}{2 + s_j\Delta t}\boldsymbol{y}_j$ ▷ Eq. (46)

compute effective stiffness $\hat{\boldsymbol{K}} = \bar{\boldsymbol{K}} + \sum \dfrac{m_j\Delta t}{2 + s_j\Delta t}\dfrac{\mathrm{d}\boldsymbol{y}_j}{\mathrm{d}\boldsymbol{u}} + \sum \dfrac{\mathrm{d}\boldsymbol{h}_j}{\mathrm{d}\boldsymbol{u}}$ ▷ Eq. (48)

compute effective resistance $\hat{\boldsymbol{r}} = \boldsymbol{r} + \sum \boldsymbol{f}_j + \sum \boldsymbol{h}_j$

compute effective load $\boldsymbol{z}$ ▷ Eq. (51) or Eq. (53)

$\delta\boldsymbol{u} = \hat{\boldsymbol{K}}^{-1}\left(\boldsymbol{z} - \hat{\boldsymbol{r}}\right)$

update and return $\boldsymbol{u} \leftarrow \boldsymbol{u} + \delta\boldsymbol{u}$

2.2. Remarks

Table 1 summarises a few special cases. The proposed damping formulations can be applied at

Table 1: selected formulations

	s_j	m_j	$\boldsymbol{y}_j$	$\boldsymbol{h}_j$	cost	remarks
	$\mathbb{C}$	$\mathbb{C}$	$\boldsymbol{u}$	$-m_j/s_j\boldsymbol{u}$	★⯪☆☆	general, guaranteed dissipation
	$\mathbb{C}$	$\mathbb{C}$	$\boldsymbol{v}$	$\boldsymbol{0}$	★⯪☆☆	identical to [31], guaranteed dissipation
	$\mathbb{C}$	$\mathbb{C}$	$\boldsymbol{a}$	$-m_j/s_j\boldsymbol{a}$	★⯪☆☆	general, guaranteed dissipation
	$\mathbb{R}$	$\mathbb{R}$	$\dot{\boldsymbol{r}}_{\boldsymbol{u}}$ (linear: $\boldsymbol{Kv}$)	$\boldsymbol{0}$	★★☆☆	identical to [32]
Eq. (41), § 1.6	$\mathbb{C}$	$\mathbb{C}$	$\dot{\boldsymbol{r}}_{\boldsymbol{u}}$ (linear: $\boldsymbol{Kv}$)	$\boldsymbol{0}$	★★⯪☆	complex extension of [32]
§ 1.7	$\mathbb{C}$	$\mathbb{C}$	$\dot{\boldsymbol{r}}_{\boldsymbol{a}}$ (linear: $\boldsymbol{M}\dot{\boldsymbol{a}}$)	$\boldsymbol{0}$	★★★★	equiv. to § 1.6 if free vibration
Eq. (40)	$\mathbb{C}$	$\mathbb{C}$	$\boldsymbol{r}_{\boldsymbol{u}}$	$-m_j/s_j\boldsymbol{r}_{\boldsymbol{u}}$	★☆☆☆	alt. form, equiv. to Eq. (41)
Eq. (42)	$\mathbb{C}$	$\mathbb{C}$	$\boldsymbol{r}_{\boldsymbol{a}}$	$-m_j/s_j\boldsymbol{r}_{\boldsymbol{a}}$	★☆☆☆	alt. form, equiv. to Eq. (41)

The reported implementation cost is intended only to indicate the relative ranking among the formulations in the table, and does not represent a quantitative or absolute measure of computational expense. More stars indicate higher implementation cost.

both the global and the element level. Consequently, the energy-dissipating forces $\boldsymbol{f}$ and $\boldsymbol{h}$ can be flexibly formulated using either node-based or element-based representations.

The proposed formulations have the following advantages.

1. They retain the size of the original problem/system.
2. The parameters s_j and m_j accept complex values, providing extra flexibility for customising the desired damping response.

3. State determination for the additional damping history $\boldsymbol{f}_j$ is local and involves only matrix–vector multiplications.
4. The consistent tangent stiffness that enables quadratic convergence can be assembled directly, for example, using different scalar weights in weighted summation if $\boldsymbol{y}_j \in \{\boldsymbol{r_u}, \boldsymbol{r_v}, \boldsymbol{r_a}\}$ or assembling additional diagonal matrices if $\boldsymbol{y}_j \in \{\boldsymbol{u}, \boldsymbol{v}, \boldsymbol{a}\}$. In problems where the mass matrix $\boldsymbol{M}$ is constant and/or lumped, the extra computational effort is minimized.
5. The reciprocal formulations are equivalent mathematically. In the absence of other energy-dissipating actions (such as conventional viscous damping), one form can be converted into another. Instead of scaling $\boldsymbol{K}$, it is possible to scale $\boldsymbol{M}$ in the equivalent form. In global time integration methods that express the equation of motion in terms of $\boldsymbol{u}$, $\boldsymbol{M}$ is already scaled by a scalar factor; therefore, the proposed contribution can be included with merely one additional scalar multiplication.

The preceding analyses assume no additional damping actions. Consequently, the derived loss stiffnesses and loss ratios hold strictly in the absence of additional velocity-dependent energy dissipation mechanisms, such as conventional viscous damping. Nonetheless, a non-trivial $\boldsymbol{C}$ is maintained in Eq. (49) to preserve structural generality.

3. Numerical Examples

3.1. A SDOF System

We consider an SDOF system with natural frequency ω_n and damping parameters m and s, following Eq. (40). The system undergoes free vibration with initial conditions $u(0) = 1$ and $\dot{u}(0) = 0$.

$$\begin{cases} \ddot{u} + \left(1 - \dfrac{m}{s}\right)\omega_n^2 u + f = 0, \\ \dot{f} = -sf + m\omega_n^2 u. \end{cases} \tag{54}$$

The following parameters are used in the numerical simulation: $\omega_n = 10$, $m = -2$, $s = 10$. In this case, the initial condition for acceleration $a\,(0) = -120$ needs to be properly assigned. How this initial condition is assigned is an implementation detail and is not discussed here. This is generally not a concern if the global time integration is self-starting.

Fig. 1 shows the displacement history of the SDOF system with various time step sizes Δt and the corresponding error convergence rate. It is clear that second-order convergence of the Newmark method used here is retained. Fig. 2 further shows the absolute error history of the SDOF system

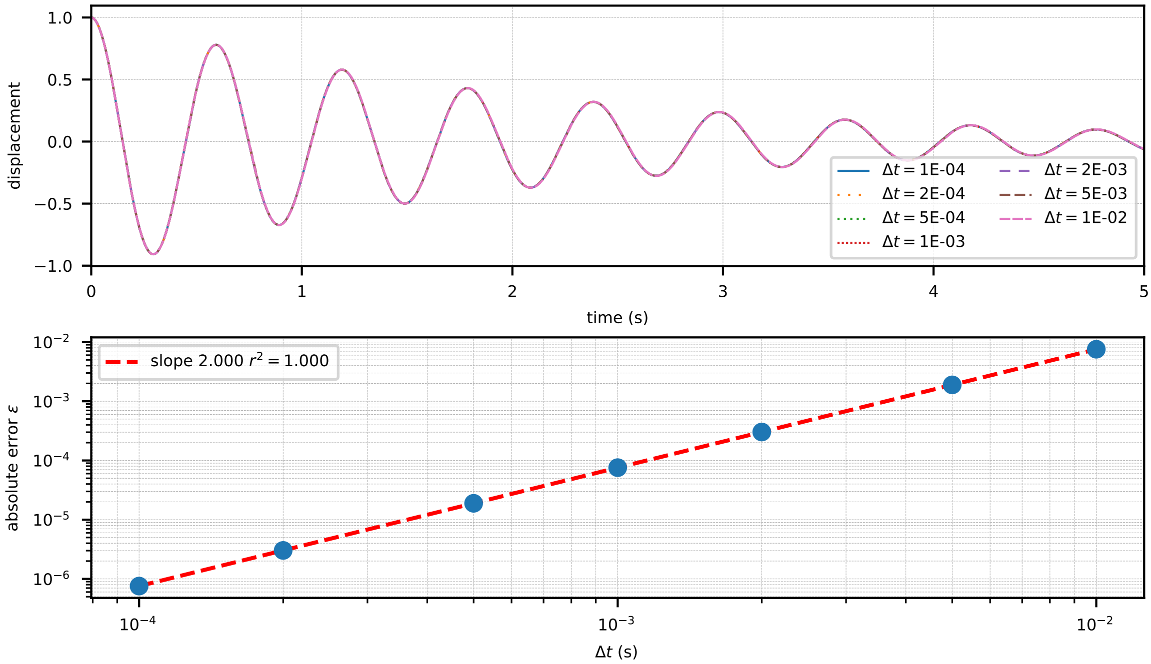

Figure 1: displacement history and error analysis of SDOF oscillator (free vibration)

in the time domain.

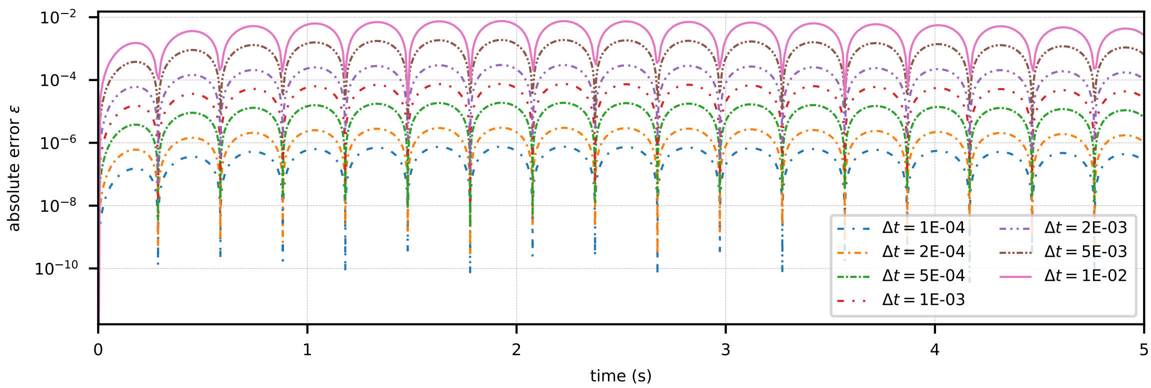

Figure 2: absolute error history of SDOF oscillator (free vibration)

One can further validate that this example can be equivalently expressed in the form of Eq. (25), with $m = 25/18$ and $s = 25/3$. To maintain brevity, these results are omitted since they are identical to those already presented.

3.2. Forced Vibration

The same SDOF system is analysed under a harmonic external load $p(t) = \sin(2\pi t)$ with trivial initial conditions. Fig. 3 and Fig. 4 show the displacement history and error convergence for formulations Eq. (40) and Eq. (42), respectively. Together, they provide further evidence that the proposed algorithm is second-order accurate for both formulations under either free or forced vibration.

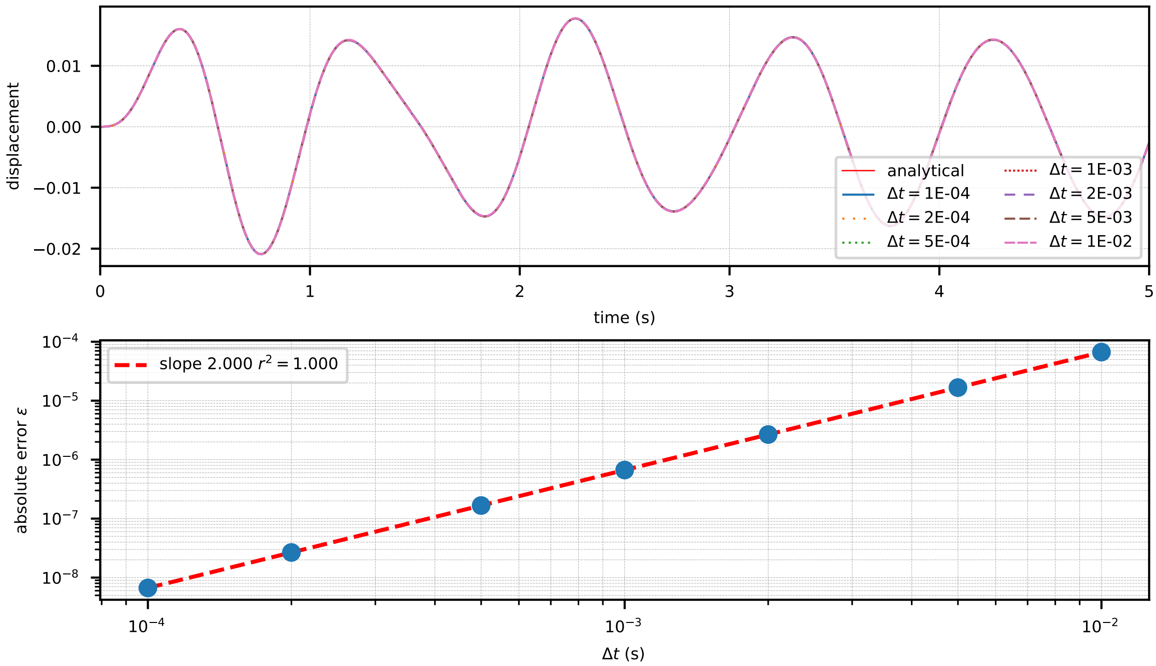

Figure 3: displacement history and error analysis of SDOF oscillator (forced vibration with UDD)

Comparing the absolute error histories in Fig. 5 and Fig. 6 shows that both formulations yield identical error histories, further confirming their equivalence under forced vibration.

3.3. Equivalence and Damping Characteristics

Although these formulations have been proven mathematically equivalent, their damping characteristics are further examined through a numerical example using the following parameters that satisfy Eq. (33). With eight terms, these parameters attempt to approximate a constant specific damping factor of 5 % from 0.1 rad/s to 100 rad/s. As shown in Fig. 7, the specific damping factor is identical in both cases. The corresponding kernel functions are, however, different (as expected).

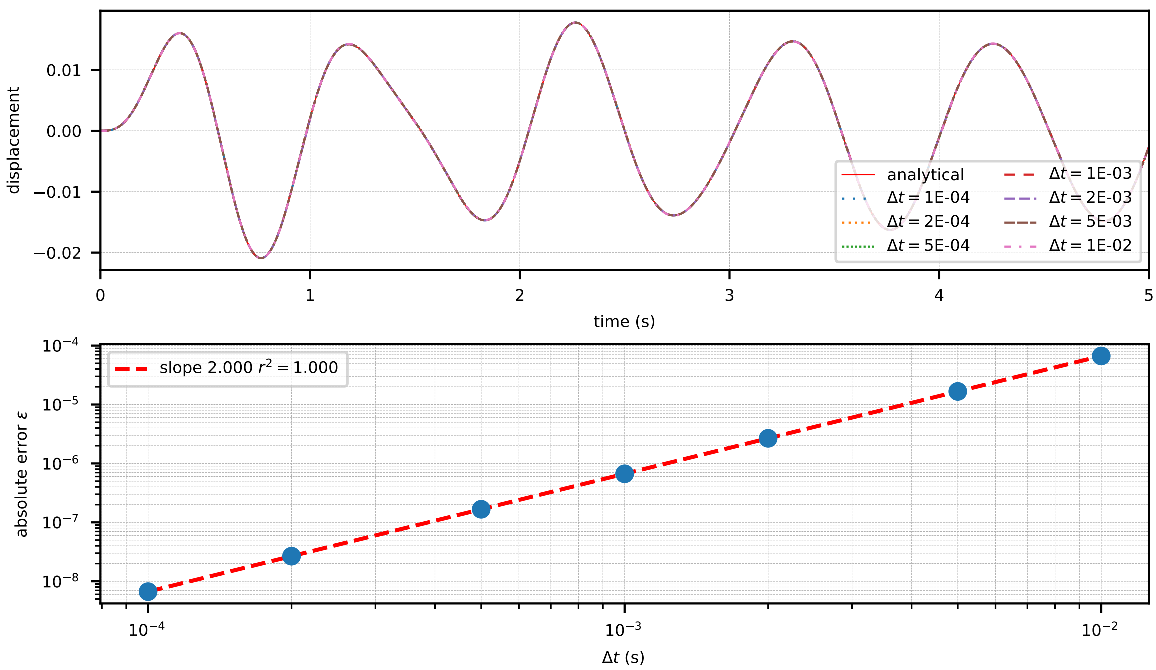

Figure 4: displacement history and error analysis of SDOF oscillator (forced vibration with UDA)

The storage stiffness gradually increases as the frequency approaches the right end of the approximation range. Outside the approximation range, it can be as high as 132 % of the static stiffness. This upper bound is controlled by the summation $\sum m_j$, which roughly corresponds to the area under the specific-damping-factor curve.

To illustrate, the following parameters are used to approximate a constant specific damping factor of 8 % with a wider approximation range from 0.001 rad/s to 1000 rad/s. As shown in Fig. 8, the storage stiffness can reach 186 % of the static stiffness above 1000 rad/s. At 1 rad/s, it is above

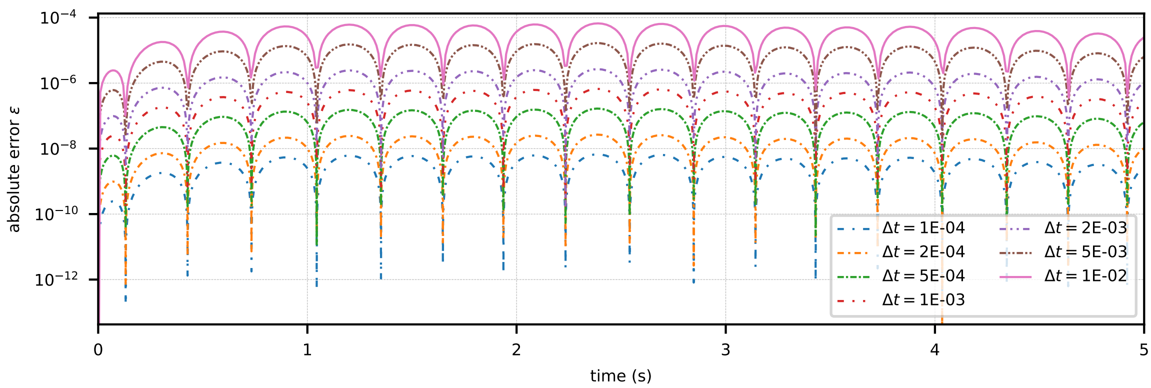

Figure 5: absolute error history of SDOF oscillator (forced vibration with UDD)

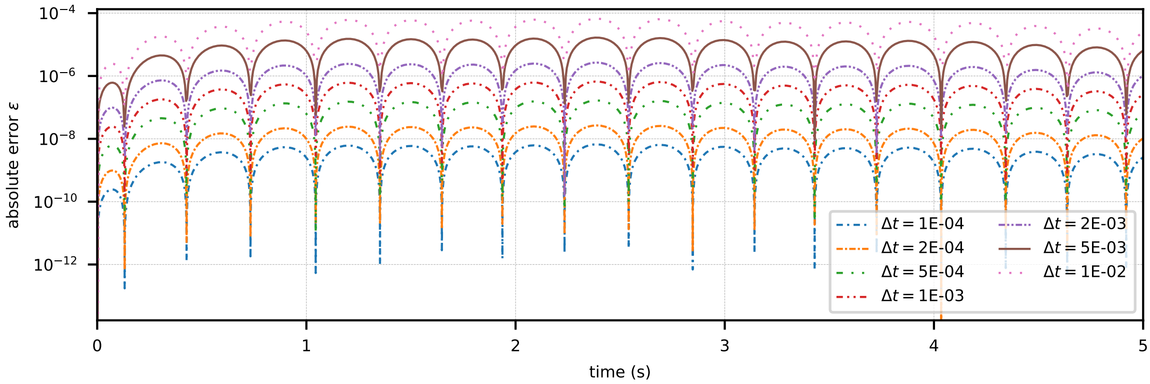

Figure 6: absolute error history of SDOF oscillator (forced vibration with UDA)

Table 2: parameter sets for the narrow-band equivalence test

m_j	s_j	m'_j	s'_j
1.7734e-02	7.9434e-02	-6.9202e-02	7.4035e-02
5.4686e-02	7.9479e-02	-8.2567e-07	7.9445e-02
3.9740e-02	3.7664e-01	-3.3311e-02	3.6317e-01
3.3290e-02	1.1730e+00	-2.6072e-02	1.1389e+00
3.0648e-02	3.1630e+00	-2.2629e-02	3.0807e+00
3.3292e-02	8.5288e+00	-2.3219e-02	8.2947e+00
3.9742e-02	2.6564e+01	-2.6073e-02	2.5722e+01
7.2414e-02	1.2589e+02	-4.2804e-02	1.1907e+02
$1+\sum m_j$	1.3215e+00		

140 % of the static stiffness.

The dynamic hardening observed at high frequencies depends on both the approximation range and the damping level. A moderately high damping level combined with a wide approximation range results in a substantial increase in storage stiffness at high frequencies.

In structural and mechanical engineering applications, the practical frequency range of interest is typically between 0.1 rad/s and 100 rad/s, spanning approximately three orders of magnitude. To accurately represent this range, the target system must remain lightly damped; otherwise, the storage stiffness deviates considerably from the static stiffness near the upper bound of the approximation range.

As discussed by Huang et al. [32], this type of nonviscous damping may be interpreted as a manifestation of stress relaxation in the underlying material. However, whether the associated hardening accurately represents the physical behaviour of the system or material remains an open question requiring further investigation.

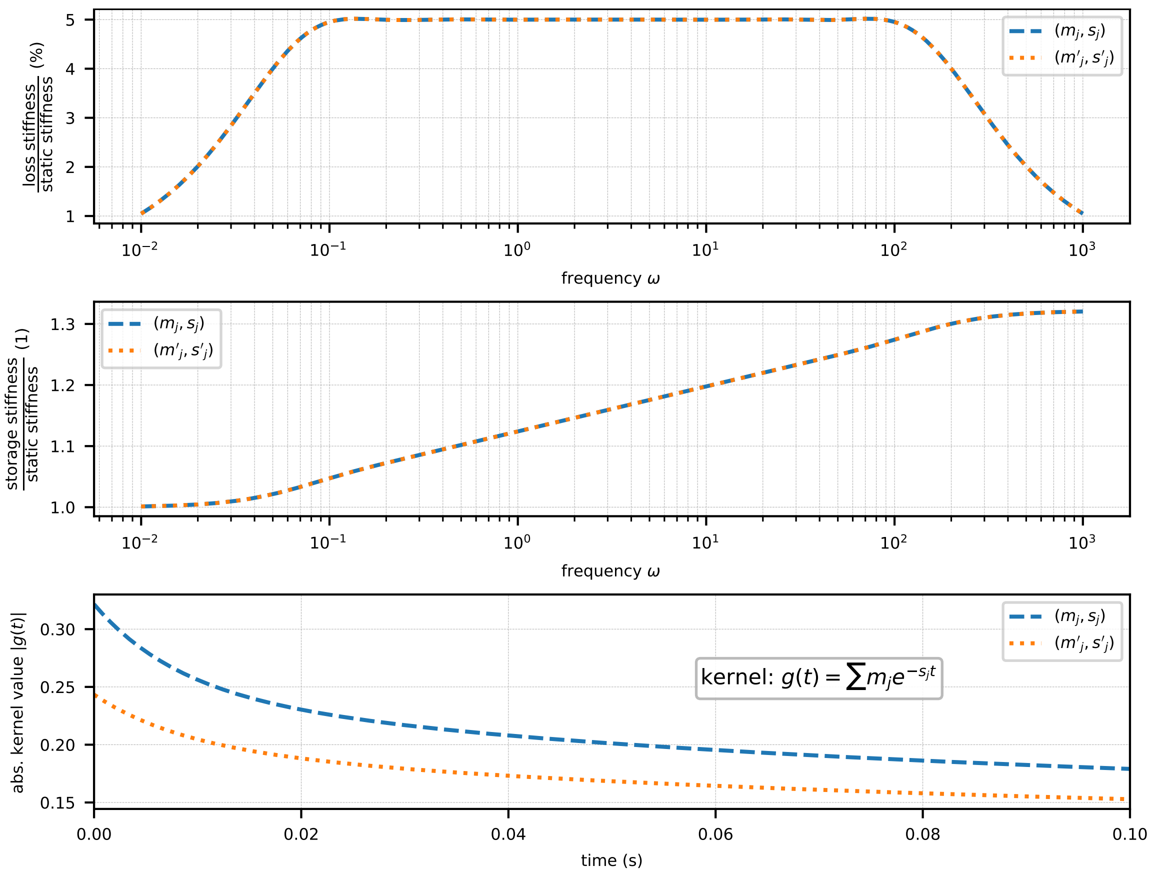

Figure 7: equivalence between formulations § 1.6 and § 1.7 with a narrow approximation range

To close this example, we further present a multi-level damping curve in Fig. 9 with higher damping levels at ultra-low and ultra-high frequencies, while maintaining a constant specific damping factor of 5 % in the middle frequency range. The corresponding parameters are not listed here for brevity.

3.4. Large System Performance

In this example, differences in performance among the proposed formulations are demonstrated. The system under consideration is a three-dimensional model comprising 20 124 nodes, each with six degrees of freedom, yielding a total of 120 744 degrees of freedom. The model includes 39 990 triangular shell elements. The global system adopts a banded storage format.

Fig. 10 presents a comparison of the wall-clock time required to analyse the system over 50 time steps. Each time step involves two iterations, resulting in a total of 100 iterations for each configuration. The system is additionally analysed under static loading to establish a baseline for

Table 3: parameter sets for the wide-band equivalence test

m_j	s_j	m'_j	s'_j
1.2080e-01	8.9800e-04	-1.1125e-01	7.9965e-04
7.8360e-02	5.1680e-03	-5.7784e-02	4.8311e-03
7.6534e-02	2.3466e-02	-4.9538e-02	2.2063e-02
7.6428e-02	1.0530e-01	-4.3917e-02	9.9369e-02
7.6424e-02	4.7224e-01	-3.9253e-02	4.4704e-01
7.6426e-02	2.1177e+00	-3.5296e-02	2.0104e+00
7.6430e-02	9.4972e+00	-3.1907e-02	9.0392e+00
7.6534e-02	4.2620e+01	-2.9018e-02	4.0656e+01
7.8358e-02	1.9352e+02	-2.7040e-02	1.8481e+02
1.2079e-01	1.1138e+03	-3.6524e-02	1.0422e+03
$1+\sum m_j$	1.8571e+00		

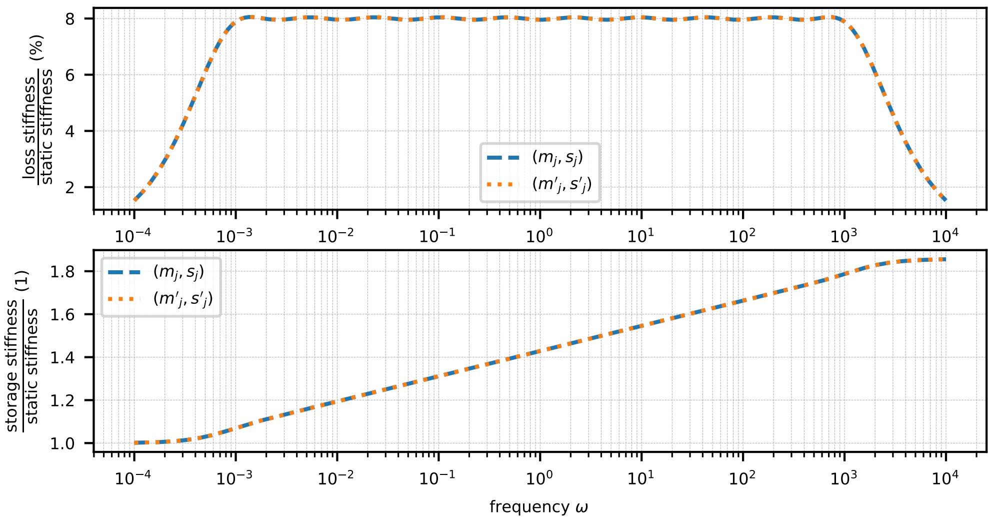

Figure 8: equivalence between formulations § 1.6 and § 1.7 with a wide approximation range

comparison. Relative to the static case, dynamic analyses primarily incur additional computational cost due to the assembly of the damping and mass matrices, as well as the corresponding effective stiffness matrix. This is reflected in the undamped case solved using the Newmark integration scheme.

For the damped analyses, the same eight terms listed in Table 2 are adopted. The label 'UDD' corresponds to the formulation in Eq. (40). In the numerical implementation, the entire system $\hat{\boldsymbol{K}}\delta\boldsymbol{u} = \boldsymbol{z} - \hat{\boldsymbol{r}}$ is rescaled such that the tangent stiffness matrix $\boldsymbol{K}$ remains unscaled, thereby achieving optimal computational performance. As shown in Fig. 10, its computational cost is virtually identical to that of the undamped case, as expected, since the additional overhead mainly

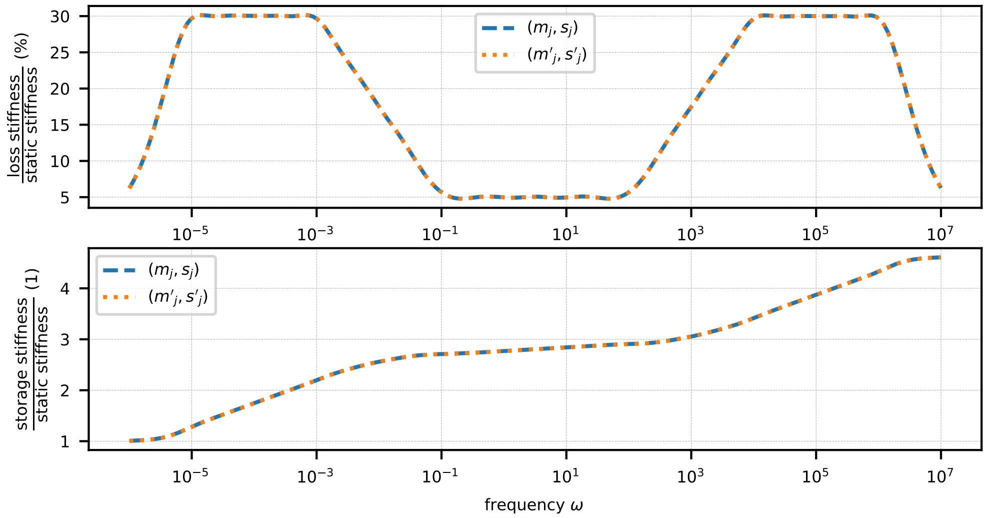

Figure 9: equivalence between formulations § 1.6 and § 1.7 with a multi-level damping curve

stems from the computation of the internal forces $\boldsymbol{f}_j$, which is computationally inexpensive. If an implementation strictly follows Eq. (48), the corresponding computational cost is expected to be higher, since the dominant additional overhead would arise from the assembly of the effective stiffness matrix, which requires scaling of the stiffness matrix. The label 'UDA' refers to the formulation in Eq. (42), for which the computational cost is only marginally higher than that of the undamped case. This behaviour is expected, as the additional cost primarily originates from the computation of the vectors $\boldsymbol{f}_j$ and $\boldsymbol{q}_j$, which scales with the number of terms employed in the analysis. For a small number of terms, the associated overhead remains negligible. Although Eq. (41) provides an analytically concise formulation, it is neither implemented nor presented owing to its evident computational inefficiency.

For large-scale problems, incorporating this form of nonviscous damping is computationally comparable to Rayleigh damping, provided that the number of pairs (m_j, s_j) remains significantly smaller than the system size. The advantage is therefore evident: the damping characteristics of the system can be tailored over a wide frequency range without significant additional computational cost.

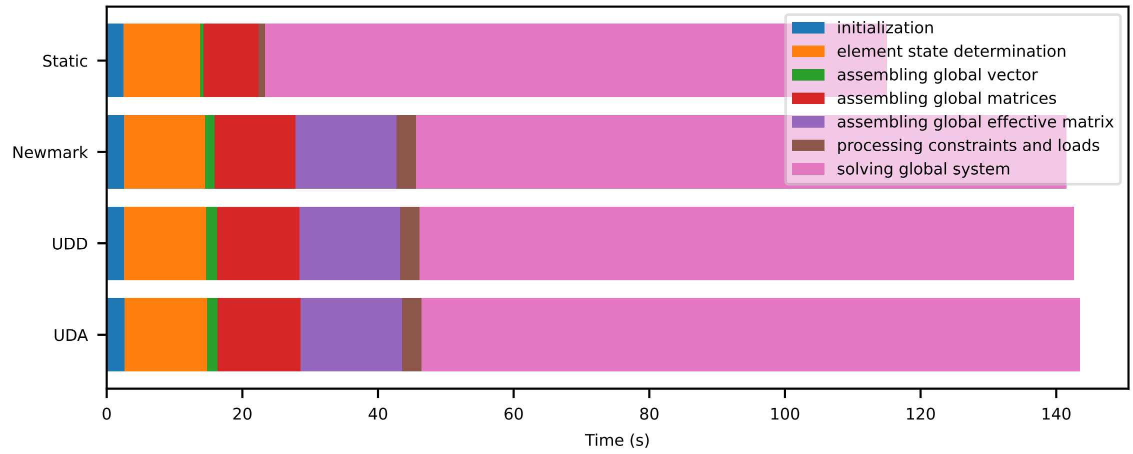

Figure 10: performance comparison among different configurations

4. Conclusions

This work has presented a general framework for constructing nonviscous damping models through additive energy-dissipating forces governed by first-order differential equations. By selecting different driving fields, several displacement-, velocity-, and acceleration-dependent formulations can be obtained within the same mathematical setting. The frequency-domain analysis identifies the associated storage and loss stiffnesses, the stability and dissipation requirements, and the role of complex conjugate parameter pairs in broadening the admissible damping response.

The main conclusions are as follows.

- Direct displacement- and acceleration-dependent formulations require algebraic correction terms to recover the correct static stiffness at low frequencies. With these corrections, the formulations remain consistent with the underlying static problem while retaining the desired dissipative behaviour.

- Three practical formulations, Eq. (40), Eq. (41) and Eq. (42), are equivalent in the frequency domain when the damping parameters are properly transformed. In the absence of additional damping mechanisms, they therefore produce the same storage and loss stiffnesses and the same dynamic response.

- The velocity-dependent formulation in Eq. (41) extends the model proposed by Huang et al. [32], but incurs higher computational cost due to the evaluation of stiffness-weighted velocity terms. In contrast, the equivalent displacement- and acceleration-based formulations avoid this operation and are therefore computationally more efficient.

- The governing equations can also be interpreted in convolution form through Eq. (39), linking the proposed differential representation to kernel-based descriptions of nonviscous damping. This interpretation provides a useful route for designing damping kernels and fitting target damping characteristics.

- The trapezoidal update of the damping history variables can be embedded into standard direct integration procedures without enlarging the global system. The resulting residual and consistent tangent effective stiffness require only additional matrix–vector operations or simple scaled matrix contributions for the practical formulations considered here.

The numerical examples confirm the analytical equivalence of selected formulations under free and forced vibration, demonstrate second-order convergence of the proposed time-discrete update, and highlight the computational benefit of the proposed forms in large-scale analysis. They also show that broadband damping approximations can introduce significant changes in storage stiffness outside the target frequency range, which should be considered when selecting damping parameters for practical applications.

The presented nonviscous damping formulations are implemented in the open-source finite element analysis framework `suanPan` [33]. All numerical examples and the relevant scripts are available in this repository[1].

Appendix A. Parameter Transform

The parameter set of one system can be transformed into the corresponding parameter set of the other system between Eq. (40) and Eq. (42). The following `Python` function implements the conversion between the two parameter sets.

```python
#!/usr/bin/env python3

import numpy as np


```

[1] https://github.com/TLCFEM/nonviscous-damping

```python
def map(m, s):
    """
    Transform damping coefficients between UDD and UDA.
    """
    m, s = np.asarray(m, np.complex128), np.asarray(s, np.complex128)

    scalar = 1 - np.sum(ms := m / s)
    poles, ev = np.linalg.eig(np.diag(s) * scalar + np.outer(ms, s))

    ev = ev[:, idx := np.argsort(poles)]
    poles = poles[idx]

    ms = s @ ev * np.linalg.solve(ev, ms) / (-scalar * poles)
    s = poles / scalar

    return ms * s, s


if __name__ == "__main__":
    print(map([-2], [10]))
```

Appendix B. Analytical Solution

Consider the SDOF system following Eq. (40) under free vibration, with ω_n denoting the natural frequency, the equation of motion after eliminating f can be expressed as

$$\dddot{u}+s\ddot{u}+\left(1-\dfrac{m}{s}\right)\omega_n^2\dot{u}+s\omega_n^2u=0. \tag{B.1}$$

Assuming $f_0=0$ gives $a_0=\left(\dfrac{m}{s}-1\right)\omega_n^2u_0$, where subscript $(\cdot)_0$ denotes initial condition. Apply the Laplace transform with $U=U\left(l\right)$ where l denotes the Laplace variable,

$$\left(l^3+sl^2+\left(1-\dfrac{m}{s}\right)\omega_n^2l+s\omega_n^2\right)U=u_0l^2+\left(su_0+v_0\right)l+sv_0. \tag{B.2}$$

The three roots of the characteristic equation $l^3+sl^2+\left(1-\dfrac{m}{s}\right)\omega_n^2l+s\omega_n^2=0$ are denoted by r_1, r_2 and r_3, so that U can be expressed as

$$U\left(l\right)=\sum_{i=1}^{3}\dfrac{P_i}{l-r_i}. \tag{B.3}$$

After expanding and comparing coefficients, one obtains

$$\begin{bmatrix} 1 & 1 & 1 \\ -r_2 - r_3 & -r_1 - r_3 & -r_1 - r_2 \\ r_2 r_3 & r_1 r_3 & r_1 r_2 \end{bmatrix} \begin{bmatrix} P_1 \\ P_2 \\ P_3 \end{bmatrix} = \begin{bmatrix} u_0 \\ s u_0 + v_0 \\ s v_0 \end{bmatrix} . \tag{B.4}$$

After solving for P_i, transforming U back to the time domain gives the solution

$$u(t) = \sum_{i=1}^{3} P_i \exp\left(r_i t\right) . \tag{B.5}$$

References

[1] PEER/ATC, Modeling and acceptance criteria for seismic design and analysis of tall buildings, Technical Report PEER/ATC 72-1, Applied Technology Council, 2010.

[2] G. G. Deierlein, A. M. Reinhorn, M. R. Willford, Nonlinear structural analysis for seismic design, Technical Report, NEHRP Seismic Design Technical Brief No. 4, 2010.

[3] J. W. S. B. Rayleigh, The theory of sound, volume 2, Macmillan, 1896.

[4] D. J. Chrisp, Damping models for inelastic structures, Master's thesis, University of Canterbury, Christchurch, New Zealand, 1980.

[5] P.-S. B. Shing, S. A. Mahin, Elimination of spurious higher-mode response in pseudodynamic tests, Earthquake engineering & structural dynamics 15 (1987) 425–445.

[6] P. Léger, S. Dussault, Seismic-energy dissipation in MDOF structures, Journal of Structural Engineering 118 (1992) 1251–1269.

[7] D. Bernal, Viscous damping in inelastic structural response, Journal of Structural Engineering 120 (1994) 1240–1254.

[8] A. Carr, Damping models for inelastic analyses, in: Proceedings of the 7th Asia-Pacific vibration conference, Kyongju, Korea, 1997, pp. 42–48. 9 - 13 November.

[9] J. F. Hall, Problems encountered from the use (or misuse) of Rayleigh damping, Earthquake engineering & structural dynamics 35 (2006) 525–545.

[10] A. J. Carr, Ruaumoko manual, Technical Report, University of Canterbury, Christchurch, 2007.

[11] F. A. Charney, Unintended consequences of modeling damping in structures, Journal of structural engineering 134 (2008) 581–592.

[12] P. Jehel, P. Léger, A. Ibrahimbegovic, Initial versus tangent stiffness-based Rayleigh damping in inelastic time history seismic analyses, Earthquake Engineering & Structural Dynamics 43 (2014) 467–484.

[13] A. K. Chopra, F. McKenna, Modeling viscous damping in nonlinear response history analysis of buildings for earthquake excitation, Earthquake Engineering & Structural Dynamics 45 (2016) 193–211.

[14] J. E. Luco, A. Lanzi, Numerical artifacts associated with Rayleigh and modal damping models of inelastic structures with massless coordinates, Earthquake Engineering & Structural Dynamics 48 (2019) 1491–1507. doi:https://doi.org/10.1002/eqe.3210.

[15] C.-L. Lee, Proportional viscous damping model for matching damping ratios, Engineering Structures 207 (2020) 110178. doi:https://doi.org/10.1016/j.engstruct.2020.110178.

[16] C.-L. Lee, Type 4 bell-shaped proportional damping model and energy dissipation for structures with inelastic and softening response, Computers & Structures 258 (2022) 106663. doi:https://doi.org/10.1016/j.compstruc.2021.106663.

[17] C.-L. Lee, T. L. Chang, A. J. Carr, Consistent assembly method for elemental damping, Computers & Structures 289 (2023) 107152. doi:https://doi.org/10.1016/j.compstruc.2023.107152.

[18] C.-L. Lee, Efficient proportional damping model for simulating seismic response of large-scale structures, in: M. Papadrakakis, M. Fragiadakis (Eds.), COMPDYN 2019 Proceedings, volume 3, 2019, pp. 4557–4564. doi:https://doi.org/10.7712/120119.7249.18776.

[19] C.-L. Lee, Sparse proportional viscous damping model for structures with large number of degrees of freedom, Journal of Sound and Vibration 478 (2020) 115312. doi:https://doi.org/10.1016/j.jsv.2020.115312.

[20] C.-L. Lee, Bell-shaped proportional viscous damping models with adjustable frequency bandwidth, Computers & Structures 244 (2021) 106423. doi:https://doi.org/10.1016/j.compstruc.2020.106423.

[21] C.-L. Lee, New elemental damping model for nonlinear dynamic response, in: W. Lacarbonara (Ed.), Advances in Nonlinear Dynamics, Volume I, Springer Nature Switzerland, Cham, 2024, pp. 387–397.

[22] C.-L. Lee, Can damping matrix depend on elemental or material response state?, in: 18th world conference on earthquake engineering, Milan, 2024, pp. 1–10.

[23] J. Woodhouse, Linear damping models for structural vibration, Journal of Sound and Vibration 215 (1998) 547–569. URL: https://www.sciencedirect.com/science/article/pii/S0022460X98917096. doi:https://doi.org/10.1006/jsvi.1998.1709.

[24] S. Adhikari, N. Wagner, Direct time-domain integration method for exponentially damped linear systems, Computers & structures 82 (2004) 2453–2461.

[25] S. Adhikari, On the quantification of damping model uncertainty, Journal of Sound and Vibration 306 (2007) 153–171. URL: https://www.sciencedirect.com/science/article/pii/S0022460X07003811. doi:https://doi.org/10.1016/j.jsv.2007.05.022.

[26] R. Shen, X. Qian, J. Zhou, C.-L. Lee, A time integration method based on the weak form galerkin method for non-viscous damping systems, Mechanical Systems and Signal Processing 151 (2021) 107361. doi:https://doi.org/10.1016/j.ymssp.2020.107361.

[27] R. Shen, X. Qian, J. Zhou, C.-L. Lee, A. Carr, R. Nokes, Study on experimental identification and alternative kernel functions of non-viscous damping in time domain, International Journal of Applied Mechanics (2022).

[28] R. Shen, X. Qian, J. Zhou, C.-L. Lee, Z. Zhang, Composite implicit time integration method for nonviscous damping structural dynamic system, Journal of Engineering Mechanics 149 (2023). doi:10.1061/JENMDT.EMENG-7040.

[29] R. Shen, X. Qian, J. Zhou, C.-L. Lee, Characteristics of passive vibration control for exponen-

tial non-viscous damping system: Vibration isolator and absorber, Journal of Vibration and Control 0 (2022) 10775463221130925. doi:https://doi.org/10.1177/10775463221130925.

[30] R. Shen, X. Qian, J. Zhou, C.-L. Lee, An eigensystem realization algorithm for identification of modal parameters of nonviscous damping structure system, International Journal of Structural Stability and Dynamics (2023). doi:10.1142/S0219455424500524.

[31] T. L. Chang, C.-L. Lee, A strategy for fast evaluation of nonviscously damped systems with arbitrary kernels, Mechanical Systems and Signal Processing 210 (2024) 111156. doi:10.1016/j.ymssp.2024.111156.

[32] Y. Huang, R. Sturt, M. Willford, A damping model for nonlinear dynamic analysis providing uniform damping over a frequency range, Computers & Structures 212 (2019) 101–109. doi:10.1016/j.compstruc.2018.10.016.

[33] T. L. Chang, suanpan — an open source, parallel and heterogeneous finite element analysis framework, 2026. doi:10.5281/ZENODO.1285221.